Dynamical properties of quasiparticles in a gapped graphene sheet

A. Qaiumzadeh,[1,2] F. K. Joibari,[2] and Reza Asgari[2]

[1]*Institute for Advanced Studies in Basic Sciences (IASBS), Zanjan, 45195-1159, Iran*
[2]*School of Physics, Institute for research in fundamental sciences, IPM 19395-5531 Tehran, Iran*

We present numerical calculations of the impact of charge carriers-carriers interactions on the dynamical properties of quasiparticles such as renormalized velocity and quasiparticle inelastic scattering lifetime in a gapped graphene sheet. Our formalism is based on the many-body G_0W-approximation for the self-energy. We present results for the many-body renormalized velocity suppression and the renormalization constant over a broad range of energy gap values. We find that the renormalized velocity is almost independence of the carrier densities at large density regime. We also show that the quasiparticle inelastic scattering lifetime decreases by increasing the gap value. Finally, we present results for the mean free path of charge carriers suppression over the energy gap values.

PACS numbers: 71.10.Ay, 81.05.Uw, 71.45.Gm

I. INTRODUCTION

The latest rival to succeed silicon's status is graphene, a single atomic layer of graphite make a truly tiny transistor to decrease the size and to improve the operational speed of the electronic devices. Silicon lost it's brilliant electronic properties in pieces smaller than about 10nm and practically the smallest silicon chips which has been used in silicon-based electronics is 45nm. Furthermore, silicon has some limitations in speed of operations. These restrictions lead to serious challenges for the Moore's law which states that the number of transistors can be placed inexpensively on an integrated circuit has increased exponentially, doubling approximately every two years. This growth cannot be maintained forever and thus the search is on to find and use new materials which may be able to produce higher performance and better functionality.

The recent discovery[1] of graphene in 2004, and its fabrication into a field-effect transistor[1], has opened up a new field of physics and offers exciting prospects for new electronic devices and apparently possible to come over those aforementioned limitations. Graphene has instructive and unique physics with special intriguing electronic properties which has attracted remarkable attentions.[2] First, the electronic properties of graphene are improved in sizes less than 10nm . Second, the massless Dirac-like electrons move through graphene with almost near-ballistic transport behavior with less resistance because back-scattering is suppressed. Third, graphene is itself a good thermal conductor such that graphene's thermal conductivity is about $\sim 5.3\times10^3$ W/mK at room temperature which is greater than the thermal conductivity of carbon nanotubes.[3] Interestingly, the mobility of carriers in graphene is quite high and it is about 10^5 cm^2/Vs at room temperature.[4] It is important to note that the highest electron mobility recorded on the semiconductor junction H-Si(111)-vacuum FET is 8×10^3cm^2/Vs at 4.2 K or the mobility of electrons in junction Si-SiO_2(100) MOSFET systems is 25×10^3cm^2/Vs at low temperature[5], make graphene promising for different applications in devices.

Providing capability to control a type and density of charge carriers by gate voltage or by the chemical doping[6] made graphene instructive for novel nano-electronic devices. However, a gapped semiconducting behavior would be more suitable for electronic applications. There have been some proposed in literature for a gap generation in graphene due to breaking of the sublattice symmetry by some substrates (such as SiC[7], graphite[8] and boron nitride[9]), to adsorbe some molecules (such as water, ammonia[10] and CrO_3[11]), spin-orbit interaction[12] and finite size effect.[13] In case, we are interested to carry out the microscopic theory to calculate some physical quantities of gapped graphene.

Theoretical calculations of quasiparticle properties of electron in conventional two-dimensional electron liquid are performed within the framework of Landau's Fermi liquid theory[14] whose key ingredient is the quasiparticle concept

and its interactions. As applied to the electron liquid model this entails the calculation of effective quasiparticle-quasiparticle interactions which enter the many-body formalism allowing the calculation of various physical properties. A number of calculations considered different variants of the G_0W-approximation for the self-energy in two-dimensional electron gas[15,16,17,18,19,20,21] from which density, spin-polarization, and temperature dependence of quasiparticle properties are obtained.

There is a mechanism for quasiparticle scattering against quasiparticles because they interact through the Coulomb interaction. This is an inelastic process and induced a finite lifetime of the quasiparticles. The carrier lifetime in an epitaxial graphene layers grown on SiC wafers has been recently measured.[22] Since experiments carried out their measurements on graphene placed on SiC, we expect that graphene was gapped. The experimental measurements are relevant for understanding carrier intraband and interband scattering mechanisms in graphene and their impact on electronic and optical devises.[23,24]

In this paper we focus on the effect of energy gap on the renormalized velocity, the inelastic scattering lifetime of quasiparticles and the inelastic mean free path in gapped graphene sheets over the broad range of energy gap. Our formalism is based on the Landau-Fermi liquid theory incorporating the G_0W-approximation for the self-energy. These quantities are related to some important physical properties of both theoretical and practical applications such as the band structure of ARPES spectra[25], the energy dissipation rate of injected carriers[22] and the width of the quasiparticle spectral function.[26]

The contents of the paper are described briefly as follows. In Section II we discuss about our theoretical model which contains the effect of gap in the renormalized velocity of quasiparticles and the inelastic scattering lifetime τ_{in}, of gapped graphene due to electron-electron interactions by using G_0W-approximation. Our numerical results are given in Section III. Finally, Section V contains the summery and conclusions.

II. THEORETICAL MODEL

Among the methods designed to deal with the intermediate correlation effects, of particular interest for its physical appeal and elegance is Landau's phenomenological theory[14] dealing with low-lying excitations in a Fermi-liquid. Landau called such single-particle excitations quasiparticles and postulated a one-to-one correspondence between them and the excited states of a non-interacting Fermi gas. He wrote the excitation energy of the Fermi-liquid in terms of the energies of the quasiparticles and of their effective interaction. The quasiparticle-quasiparticle interaction function can in turn be used to obtain various physical properties of the system and can be parameterized in terms of experimentally measurable data. In this paper, we will compute the energy gap dependence of the renormalized velocity, renormalization constant and the inelastic scattering lifetime of quasiparticle in a gapped graphene sheet.

A. Quasiparticle renormalized velocity

The dynamics of quasiparticles in a gapless graphene are described by two-dimensional (2D) massless Dirac Hamiltonian $\hat{H} = \hbar v \sigma \cdot \mathbf{k}$, with eigenvalues $\varepsilon_{s\mathbf{k}} = s\hbar vk$, where $s = +(-)$ representing right- and left-handed helicity or chirality for the electrons and holes, respectively. Note that chirality is the same as helicity for the massless particles. $v = 10^6$ m/s is the Fermi velocity. As it has been shown before[27], contrary to conventional 2D electron systems, the interactions increase the velocity of quasiparticles in graphene because of interband exchange interactions and the difference between positive and negative energy branches due to the chirality.

The dynamics of quasiparticles in a gapped graphene are described by 2D massive Dirac Hamiltonian given by $\hat{H} = \hbar v_F \sigma \cdot \mathbf{k} + mv^2\sigma_3$ with eigenvalues $E_{s\mathbf{k}} = s\sqrt{(\hbar vk)^2 + \Delta^2}$ where $\Delta = mv^2$ is the gap energy. Due to massive term

in the Hamiltonian, the chirality differs from the helicity and also the helicity is conserved but is frame dependence.

From the microscopic point of view, the quasiparticle energy can be calculated by solving the Dyson equation,

$$\delta\varepsilon^{QP}_{s\mathbf{k}} = \xi_{s\mathbf{k}} + \Re e[\delta\Sigma^{ret}_s(\mathbf{k},\omega)]|_{\omega=\delta\varepsilon^{QP}_{s\mathbf{k}}/\hbar}, \tag{1}$$

where $\xi_{s\mathbf{k}} = E_{s\mathbf{k}} - E_{\rm F}$ is the energy of a quasiparticle relative to the Fermi energy. The Fermi wave vector in graphene is given by $k_{\rm F} = (4\pi n/g_s g_v)^{1/2}$ where $g_s = g_v = 2$ are spin and valley degeneracy, respectively. The Fermi energy of gapless graphene is $\varepsilon_{\rm F} = \hbar v k_{\rm F}$. The retarded self-energy of gapped graphene is Σ^{ret}_s and we define $\delta\Sigma^{ret}_s(\mathbf{k},\omega) = \Sigma^{ret}_s(\mathbf{k},\omega) - \Sigma^{ret}_s(k_F,0)$. In the on-shell approximation[28], on the other hand, the above equation must be solved by setting $\omega = \xi_{s\mathbf{k}}/\hbar$.

In the G_0W- approximation[28], the self-energy of gapped graphene at finite temperature ($\beta = 1/(k_B T)$) is given by

$$\begin{aligned}\Sigma_s(\mathbf{k}, i\omega_n) &= -\frac{1}{\beta}\sum_{s'}\int \frac{d^2\mathbf{q}}{(2\pi)^2} F^{ss'}(\mathbf{k},\mathbf{k}+\mathbf{q}) \\ &\times \sum_{m=-\infty}^{+\infty} W(\mathbf{q}, i\Omega_m) G^{(0)}_{s'}(\mathbf{k}+\mathbf{q}, i\omega_n + i\Omega_m),\end{aligned} \tag{2}$$

where the dynamic screened effective interaction is $W(\mathbf{q}, i\Omega_m) = V_q/\epsilon(q, i\Omega_m)$ and $\epsilon(q, i\Omega_m)$ is the dynamical dielectric function and the bare Coulomb interaction is $V_q = 2\pi e^2/\kappa q$ where κ is the averaged background dielectric constant of graphene is placed on a substrate. $G^{(0)}_s(q, i\Omega_m) = 1/(i\Omega_m - \xi_{s\mathbf{k}}/\hbar)$ is the standard noninteracting Green's function. The overlap function for gapped graphene $F^{ss'}(\mathbf{k},\mathbf{k}+\mathbf{q})$, is given by[29]

$$F^{ss'}(\mathbf{k},\mathbf{k}+\mathbf{q}) = \frac{1}{2}(1 + ss'\frac{\hbar^2 v^2 \mathbf{k}\cdot(\mathbf{k}+\mathbf{q}) + \Delta^2}{E_{\mathbf{k}} E_{\mathbf{k}+\mathbf{q}}}) \ . \tag{3}$$

To evaluate of the zero temperature retarded self-energy, we decompose the self-energy into the line which is purely a real function and residue contributions, $\Sigma^{ret}_s(\mathbf{k},\omega) = \Sigma^{line}_s(\mathbf{k},\omega) + \Sigma^{res}_s(\mathbf{k},\omega)$, where Σ^{line} is obtained by performing the analytic continuation before summing over the Matsubara frequencies, and Σ^{res} is the correction which must be taken into account in the total self-energy,

$$\begin{aligned}\Sigma^{line}_s(\mathbf{k},\omega) &= -\sum_{s'}\int \frac{d^2\mathbf{q}}{(2\pi)^2} V_q F^{ss'}(\mathbf{k},\mathbf{k}+\mathbf{q}) \\ &\times \int_{-\infty}^{\infty}\frac{d\Omega}{2\pi}\frac{1}{\epsilon(\mathbf{q}, i\Omega)}\frac{1}{\omega + i\Omega - \xi_{s'}(\mathbf{k}+\mathbf{q})/\hbar},\end{aligned} \tag{4}$$

and

$$\begin{aligned}\Sigma^{res}_s(\mathbf{k},\omega) &= \sum_{s'}\int \frac{d^2\mathbf{q}}{(2\pi)^2}\frac{V_q}{\epsilon(\mathbf{q}, \omega - \xi_{s'}(\mathbf{k}+\mathbf{q})/\hbar)} F^{ss'}(\mathbf{k},\mathbf{k}+\mathbf{q}) \\ &\times \ [\Theta(\omega - \xi_{s'}(\mathbf{k}+\mathbf{q})/\hbar) - \Theta(-\xi_{s'}(\mathbf{k}+\mathbf{q})/\hbar)],\end{aligned} \tag{5}$$

where the dynamic dielectric function is given by $\epsilon(\mathbf{q},\omega) = 1 - V_q\chi^{(0)}(q,\omega)$ in the random phase approximation (RPA) and $\chi^{(0)}(q,\omega)$ is the noninteracting polarization function for gapped graphene. The noninteracting polarization function has been recently calculated on both along the imaginary and real frequency axis[29,30]. The noninteracting polarization function expressions along the real frequency axis[30] are given in appendix A.

Note that there are two independent parameters in the self-energy. One of them is the Fermi energy $E_{\rm F}$, and the other is the dimensionless coupling constant $\alpha_{gr} = g_s g_v e^2/\kappa\hbar v$. The coupling constant in graphene depends only on the substrate dielectric constant while in the conventional 2D electron systems the coupling constant is density dependent. For graphene placed on SiC or graphite substrates, the coupling constant is about $\alpha_{gr} \simeq 1$.

The quasiparticle energy depends on the magnitude of $\mathbf{k}$ for the isotropic systems. Expanding $\delta\varepsilon^{QP}_{+k}$ to first order in $k-k_{\rm F}$, we obtain $\delta\varepsilon^{QP}_{+k} \simeq \hbar v^*(k-k_{\rm F})$ which effectively defines the renormalized velocity as $\hbar v^* = d\delta\varepsilon^{QP}_{+k}/dk|_{k=k_{\rm F}}$. The renormalized velocity in the Dyson scheme is thus given by

$$\frac{v^*}{v} = \frac{(1+\Delta^2)^{-1/2} + v^{-1}\partial_k \Re e[\delta\Sigma^{ret}_+(\mathbf{k},\omega)]|_{\omega=0,k=k_{\rm F}}}{1-\partial_\omega \Re e[\delta\Sigma^{ret}_+(\mathbf{k},\omega)]|_{\omega=0,k=k_{\rm F}}} \; . \tag{6}$$

In the on-shell approximation, on the other hand, the renormalized velocity is given by $v^*/v = (1+\Delta^2)^{-1/2} + v^{-1}\partial_k \Re e[\delta\Sigma^{ret}_+(\mathbf{k},\omega)]|_{\omega=0,k=k_{\rm F}} + (1+\Delta^2)^{-1/2}\partial_\omega \Re e[\delta\Sigma^{ret}_+(\mathbf{k},\omega)]|_{\omega=0,k=k_{\rm F}}$. The renormalized velocity in this approximation demonstrates qualitatively the same behavior obtained by the Dyson equation, Eq. (6) but its magnitude is larger than the one calculated within the Dyson scheme.[20] There is an ultraviolet divergence in the wave vector integrals of the line contribution in a continuum model formulated as discussed above.[27] We introduce an ultraviolet cutoff for the wave vector integrals, $k_c = \Lambda k_F$ which is the order of the inverse lattice spacing and Λ is dimensionless quantity. For definiteness we take $\Lambda = k_c/k_F$ to be such that $\pi(\Lambda k_F)^2 = (2\pi)^2/\mathcal{A}_0$, where $\mathcal{A}_0 = 3\sqrt{3}a_0^2/2$ is the area of the unit cell in the honeycomb lattice, with $a_0 \simeq 1.42$ Å the carbon-carbon distance. With this choice, $\Lambda \simeq (gn^{-1}\sqrt{3}/9.09)^{1/2}\times 10^2$, where n is the electron density in units of 10^{12} cm^{-2}.

An important quantity in the Fermi-liquid theory is the renormalization constant Z, defined as the square of the overlap between the state of the system after adding (or removing) of an electron with the Fermi wave vector and the ground-state of the system. The non-zero renormalization constant value is always smaller than the one for the normal Fermi-liquid systems and can be calculated explicitly as follow[28]

$$Z = \frac{1}{1-\partial_\omega \Re e[\delta\Sigma^{ret}_+(\mathbf{k},\omega)]|_{\omega=0,k=k_{\rm F}}}. \tag{7}$$

We will show that Z is a finite number for gapped graphene and it confirms as well that the system is a Fermi-Liquid.

B. Inelastic scattering lifetime

In this subsection, we compute the inelastic scattering lifetime of quasiparticles due to carriers-carriers interactions at zero temperature and disorder-free for gapped graphene sheets. This is obtained through the imaginary part of the self-energy[31] when the frequency evaluated at the on-shell energy.

$$\tau^{-1}_{in}(\mathbf{k}) = \Gamma_{in}(\mathbf{k},\xi_{+\mathbf{k}}/\hbar) = -\frac{2}{\hbar}\Im m\Sigma^{ret}_+(\mathbf{k},\xi_{+\mathbf{k}}/\hbar), \tag{8}$$

where $\Gamma_{in}(\mathbf{k},\xi_{s\mathbf{k}}/\hbar)$ is the quantum level broadening of the momentum with eigenstate $|s\mathbf{k}>$. It is worthwhile to note that the expression of τ^{-1}_{in} is identical with a result obtained by the Fermi's golden rule summing the scattering rate of electron and hole contributions at wave vector $\mathbf{k}$.[28] Note again that the total contribution of the imaginary part of the retarded self-energy comes from the residue term both intra- and interband contributions, $\Im m\Sigma^{ret}_+(\mathbf{k},\omega) = \Im m\Sigma^{res}_{intra}(\mathbf{k},\omega) + \Im m\Sigma^{res}_{inter}(\mathbf{k},\omega)$. However, the total contribution of the imaginary part of the retarded self-energy evaluated at the on-shell energy comes only from intraband term, $\Im m\Sigma^{ret}_+(\mathbf{k},\xi_{\mathbf{k}}/\hbar) = \Im m\Sigma^{res}_{intra}(\mathbf{k},\xi_{\mathbf{k}}/\hbar)$. We will discuss about that with more details in the appendix B and C.

We turn our attention to investigate the imaginary part of the retarded self-energy with more details. By starting

from Eq. (5), we end up to an expression for the imaginary part of self-energy which is given by,

$$\begin{aligned}
\Im m\Sigma_{+}^{ret}(\mathbf{k},\omega) &= \Im m\Sigma_{intra}^{res}(\mathbf{k},\omega) + \Im m\Sigma_{inter}^{res}(\mathbf{k},\omega) \\
&= \int \frac{d^2\mathbf{q}}{(2\pi)^2} V_q \Im m[\epsilon^{-1}(\mathbf{q},\omega-\xi_+(\mathbf{k}+\mathbf{q})/\hbar)] F^{++}(\mathbf{k},\mathbf{k}+\mathbf{q}) \\
&\times [\Theta(\omega-\xi_+(\mathbf{k}+\mathbf{q})/\hbar) - \Theta(-\xi_+(\mathbf{k}+\mathbf{q})/\hbar)] \\
&+ \int \frac{d^2\mathbf{q}}{(2\pi)^2} V_q \Im m[\epsilon^{-1}(\mathbf{q},\omega-\xi_-(\mathbf{k}+\mathbf{q})/\hbar)] F^{+-}(\mathbf{k},\mathbf{k}+\mathbf{q}) \\
&\times [\Theta(\omega-\xi_-(\mathbf{k}+\mathbf{q})/\hbar) - \Theta(-\xi_-(\mathbf{k}+\mathbf{q})/\hbar)]. \qquad (9)
\end{aligned}$$

where the imaginary part of the inverse dielectric function in RPA level is obtained by

$$\Im m[\epsilon^{-1}(\mathbf{q},\omega)] = \frac{V_q \Im m\chi^{(0)}(\mathbf{q},\omega)}{[1-V_q \Re e\chi^{(0)}(\mathbf{q},\omega)]^2 + [V_q \Im m\chi^{(0)}(\mathbf{q},\omega)]^2}. \qquad (10)$$

It is worth to note that the plasmon contributions in the imaginary part of self-energy comes from the zero-solutions of denominator in Eq. (10).

III. NUMERICAL RESULTS

We turn to a presentation of our main numerical results. We present some illustrative results for the quasiparticle dynamic properties such renormalized velocity, renormalization constant and inelastic scattering lifetime. All numerical data are calculated in the Dyson scheme at $\alpha = 1$.

The Fermi liquid phenomenology of Dirac electrons in gapless graphene[25,27] and conventional 2D electron liquid[20] have the same structure, since both systems are isotropic and have a single circular Fermi surface. The strength of interaction effects in a conventional 2D electron liquid increases with decreasing carrier density. At low densities, the quasiparticle renormalization constant Z is small, the renormalized velocity is suppressed[20], the charge compressibility changes sign from positive to negative, and the spin-susceptibility is strongly enhanced[32]. These effects emerge from an interplay between exchange interactions and quantum fluctuations of charge and spin in the 2D electron liquid.

In the 2D massless electron graphene, on the other hand, it has been shown[25,27,33] that interaction effects also become noticeable with decreasing density, although more slowly, the quasiparticle renormalization constant, Z tends to larger values, that the renormalized velocity is enhanced rather than suppressed, and that the influence of interactions on the compressibility and the spin-susceptibility changes sign. These qualitative differences are due to exchange interactions between electrons near the Fermi surface and electrons in the negative energy sea and to interband contributions to Dirac electrons from charge and spin fluctuations.

In this paper we have shown the results for gapped graphene which are determined values between the gapless graphene evaluated at $\triangle = 0$ and the conventional 2D electron liquid where $\triangle \to \infty$.

In Fig. 1, we have plotted the renormalized velocity as a function of carrier density for the various energy gap. As a result, we see that the impact of energy gap on quasiparticles velocity which is similar to the effect of impurity to that on graphene[34]. The renormalized velocity is almost density independent in gapped graphene at large carrier densities. The renormalized velocity reduces dramatically by increasing the energy gap especially in the low carrier densities. Importantly, the renormalized velocity becomes less than the bare velocity at large energy gap and low density values. It is physically accepted since the system tends to conventional 2D electron liquid by increasing the energy gap values. Note that in the conventional 2D electron systems, the renormalized velocity is suppressed by increasing the coupling constant or reducing the density.

We have shown the renormalization constant Z, as a function of the energy gap in Fig. 2. The renormalization constant enormously reduces by increasing the energy gap in mild densities, however it decreases quite slowly in high densities.

Fig. 3(a) is shown the absolute value of $\Im m\Sigma^{\rm ret}_{+}(\mathbf{k},\omega)$ as from Eq. (9), evaluated at $\omega = \xi_{\mathbf{k}}/\hbar$. By increasing the gap value, this function takes a finite jump at the wave number of the plasmon dip and at large $\triangle$ values, a discontinuity appears. The discontinuity is peculiar to $2D$ electron liquid.[35] It is absent in gapless graphene and starts to arise from the fact that the oscillator strength of the plasmon pole is non-zero at special k value for gapped graphene.

Fig. 3(b) is clearly shown the behavior of the energy gap dependence of the inverse inelastic scattering lifetime. As it is argued in the Appendix B, the imaginary part of self-energy evaluated at the on-shell energy start from $\triangle - \sqrt{\varepsilon_{\rm F}^2 + \triangle^2}$ and in case the results are truncated below that. The quasiparticle lifetime decreases by increasing the gap value and it is a clear difference between 2D massless Dirac electron and gapped graphene. Consequently, the inelastic scattering lifetime in graphene is always larger than the conventional 2D electron liquid. In the case of gapless graphene, scattering rate is a smooth function because of the absence of both plasmon emission and interband processes,[31] nevertheless with generating a gap and increasing the amount of it, plasmon emission causes to arise a discontinuity in the scattering time, similar to conventional 2D electron liquid.[20] We have thus two mechanisms for scattering of the quasiparticles. The excitation of electron-hole pairs which is dominant process at low wave vectors and the excitation of plasmon appears in a specific wave vector. We also see in Fig. 3(b) that the scattering rate is quite sensitive to the gap energy and the scattering rate increases by increasing the energy gap.

In Fig. 4, we have depicted the inelastic mean free path $l_{in}(\mathbf{k}) = v^*\tau_{in}(\mathbf{k})$, as a function of the on-shell energy for various gap energies. To this purpose we multiplied the results of $\tau_{in}(\mathbf{k})$ to a proper renormalized velocity. As a result the mean free path of a gapped graphene is shorter than that obtained for gapless graphene. Furthermore, the massless graphene has larger l_{in} and it decreases by increasing the energy gap values. Note that the typical value of energy gap due to breaking sublattice symmetry is $\triangle = 10 - 100$ meV corresponding the inelastic mean free path is $l_{in} = 20 - 50$ nm which implies that the system remains in the semi-ballistic regime.[7,8,9,10].

IV. SUMMERY AND CONCLUDING REMARKS

In summary, we have studied the problem of the microscopic calculation of the quasiparticle self-energy and many-body renormalized velocity suppression over the energy gap in a gapped graphene. We have carried out calculations of both the real and the imaginary part of the quasiparticle self-energy within G_0W-approximation. We have also presented results for the renormalized velocity suppression and for the renormalization constant over a wide range of energy gap. We have shown that the renormalized velocity for a gapped graphene is almost independent of the carrier density at high density. We have finally presented results for the quasiparticle inelastic scattering lifetime suppression over the energy gap and show that the mean free path of the charge carriers of a gapless graphene is larger than a gapped graphene one. In case the mean free path of charge carriers decrease by increasing the energy gap.

A possible role of correlations including the charge-density fluctuations beyond the Random Phase Approximation, remains to be examined.

Acknowledgments

R. A. would like to thank the International Center for Theoretical Physics, Trieste for its hospitality during the period when part of this work was carried out. A. Q is supported by IPM grant.

APPENDIX A: THE DYNAMIC POLARIZATION FUNCTION FOR A GAPPED GRAPHENE

In this appendix we present the real and imaginary part of the noninteracting polarization function for a gapped graphene, which is calculated recently by Pyatkovskiy.[30] The dynamic polarization function for gapped graphene in the imaginary frequency axis is also calculated by us in Ref. [29]. Importantly, the noninteracting polarization function along the imaginary frequency axis can be obtained by performing analytical continuation from real axis and those results are the same.[36]

First, by introducing some following notations,

$$\begin{aligned} f(k,\omega) &= \frac{g_s g_v k^2}{16\pi\sqrt{|\hbar^2 v^2 k^2 - \hbar^2\omega^2|}}, \\ g_\pm &= \frac{2E_{\rm F} \pm \hbar\omega}{\hbar v k}, \\ x_0 &= \sqrt{1 + \frac{4\Delta^2}{\hbar^2 v^2 k^2 - \hbar^2\omega^2}}, \\ G_<(x) &= x\sqrt{x_0^2 - x^2} - (2 - x_0^2)\cos^{-1}(x/x_0), \\ G_>(x) &= x\sqrt{x^2 - x_0^2} - (2 - x_0^2)\cosh^{-1}(x/x_0), \\ G_0(x) &= x\sqrt{x^2 - x_0^2} - (2 - x_0^2)\sinh^{-1}(x/\sqrt{-x_0^2}), \end{aligned} \tag{A1}$$

the real part of noninteracting polarization function is given by,

$$\Re e\chi^{(0)}(k,\omega) = -\frac{g_s g_v E_{\rm F}}{2\pi v_F^2} + f(k,\omega)\times \begin{cases} 0, & 1{\rm A} \\ G_<(g_-), & 2{\rm A} \\ G_<(g_+) + G_<g_-), & 3{\rm A} \\ G_<(g_-) - G_<(g_+), & 4{\rm A} \\ G_>(g_+) - G_>(g_-), & 1{\rm B} \\ G_>(g_+), & 2{\rm B} \\ G_>(g_+) - G_>(-g_-), & 3{\rm B} \\ G_>(-g_-) + G_>(g_+), & 4{\rm B} \\ G_0(g_+) - G_0(g_-), & 5{\rm B} \end{cases} \tag{A2}$$

and the imaginary part of noninteracting polarization function is given by,

$$\Im m\chi^{(0)}(k,\omega) = f(k,\omega)\times \begin{cases} G_>(g_+) - G_>(g_-), & 1{\rm A} \\ G_>(g_+), & 2{\rm A} \\ 0, & 3{\rm A} \\ 0, & 4{\rm A} \\ 0, & 1{\rm B} \\ -G_<(g_-), & 2{\rm B} \\ \pi(2 - x_0^2), & 3{\rm B} \\ \pi(2 - x_0^2), & 4{\rm B} \\ 0, & 5{\rm B} \end{cases} \tag{A3}$$

with the followings regions in the (k,ω) space,

$$\begin{array}{ll} 1A & \hbar\omega < E_{\rm F} - \sqrt{\hbar^2 v^2 (k - k_{\rm F})^2 + \Delta^2}, \\ 2A & |E_{\rm F} - \sqrt{\hbar^2 v_F^2 (k - k_{\rm F})^2 + \Delta^2}| < \hbar\omega < -E_{\rm F} + \sqrt{\hbar^2 v^2 (k + k_{\rm F})^2 + \Delta^2}, \\ 3A & \hbar\omega < -E_{\rm F} + \sqrt{\hbar^2 v^2 (k - k_{\rm F})^2 + \Delta^2}, \\ 4A & -E_{\rm F} + \sqrt{\hbar^2 v^2 (k + k_{\rm F})^2 + \Delta^2} < \hbar\omega < \hbar v k, \\ 1B & k < 2k_{\rm F}, \quad \sqrt{\hbar^2 v^2 k^2 + 4\Delta^2} < \hbar\omega < E_{\rm F} + \sqrt{\hbar^2 v^2 (k - k_{\rm F})^2 + \Delta^2}, \\ 2B & E_{\rm F} + \sqrt{\hbar^2 v^2 (k - k_{\rm F})^2 + \Delta^2} < \hbar\omega < E_{\rm F} + \sqrt{\hbar^2 v^2 (k + k_{\rm F})^2 + \Delta^2}, \\ 3B & \hbar\omega > E_{\rm F} + \sqrt{\hbar^2 v^2 (k + k_{\rm F})^2 + \Delta^2}, \\ 4B & k > 2k_{\rm F}, \quad \sqrt{\hbar^2 v^2 k^2 + 4\Delta^2} < \hbar\omega < E_{\rm F} + \sqrt{\hbar^2 v^2 (k - k_{\rm F})^2 + \Delta^2}, \\ 5B & \hbar v k < \hbar\omega < \sqrt{\hbar^2 v^2 k^2 + 4\Delta^2}, \end{array} \tag{A4}$$

APPENDIX B: THE INTRABAND CONTRIBUTION OF SELF-ENERGY

Since we are interested in quasiparticle properties, we therefore need only $s = +$ contribution. Let us focus on the intraband contribution of the retarded self-energy. The second argument of the dielectric function in Eq. (5) (by setting $\hbar = v = 1$) is

$$\omega - \xi_+(\mathbf{k}+\mathbf{q}) = \omega + E_{\rm F} - \sqrt{k^2+q^2+2kq\cos\phi+\Delta^2}\ . \tag{B1}$$

In this case, we change the variable ϕ and integrate it over $y = \sqrt{k^2+q^2+2kq\cos\phi+\Delta^2}$. Using the new variable, the intraband contribution of self-energy changes to

$$\begin{aligned}\Sigma^{res}_{intra}(\mathbf{k},\omega) &= \frac{e^2}{2\pi\kappa\sqrt{k^2+\Delta^2}}\int_0^{+\infty} dq \int_{\sqrt{(k-q)^2+\Delta^2}}^{\sqrt{(k+q)^2+\Delta^2}} \frac{dy}{\sqrt{4k^2q^2-(y^2-k^2-q^2-\Delta^2)^2}} \frac{(\sqrt{k^2+\Delta^2}+y)^2-q^2}{\epsilon(\mathbf{q},\omega+E_{\rm F}-y)} \\ &\times\ [\Theta(\omega+E_{\rm F}-y)-\Theta(E_{\rm F}-y)].\end{aligned} \tag{B2}$$

We can now simplify the Θ-functions further in Eq. (B2) by considering the positive and negative regions of ω as follow

$$\begin{aligned}&1)\ \ \omega\ \ +E_{\rm F}-y>0\ and\ \ E_{\rm F}-y<0:\ \ It\ implies\ that\ \omega>0\ ,\\ &2)\ \ \omega\ \ +E_{\rm F}-y<0\ and\ \ E_{\rm F}-y>0:\ \ It\ implies\ that\ \omega<0\ .\end{aligned}$$

To consider the first case where $\omega > 0$, the difference between the two Θ-functions in Eq. (B2) is equal to $+1$ if

$$E_{\rm F} < y < \omega + E_{\rm F}\ \ and\ \ \sqrt{(k-q)^2+\Delta^2} < y < \sqrt{(k+q)^2+\Delta^2}\ . \tag{B3}$$

Now we do need to find the overlap between these two intervals. We simply end up to inequivalent conditions which are $q > k - \sqrt{\omega^2+k_{\rm F}^2+2\omega\sqrt{k_{\rm F}^2+\Delta^2}}$, $q < k + \sqrt{\omega^2+k_{\rm F}^2+2\omega\sqrt{k_{\rm F}^2+\Delta^2}}$ and $q > k_{\rm F} - k$. Collecting everything together and using the fact that $q \geq 0$, we finally find

$$\begin{aligned}\Sigma^{res}_{intra}(\mathbf{k},\omega>0) &= \frac{e^2}{2\pi\kappa\sqrt{k^2+\Delta^2}}\int_{max(0,k_{\rm F}-k,k-\sqrt{\omega^2+k_{\rm F}^2+2\omega\sqrt{k_{\rm F}^2+\Delta^2}})}^{k+\sqrt{\omega^2+k_{\rm F}^2+2\omega\sqrt{k_{\rm F}^2+\Delta^2}}} dq \int_{max(\sqrt{k_{\rm F}^2+\Delta^2},\sqrt{(k-q)^2+\Delta^2})}^{min(\omega+\sqrt{k_{\rm F}^2+\Delta^2},\sqrt{(k+q)^2+\Delta^2})} dy \\ &\times\ \frac{(\sqrt{k^2+\Delta^2}+y)^2-q^2}{\epsilon(\mathbf{q},\omega+E_{\rm F}-y)\sqrt{4k^2q^2-(y^2-k^2-q^2-\Delta^2)^2}}\end{aligned} \tag{B4}$$

By considering of the second case where $\omega < 0$, the difference between the two Θ-functions in Eq. (5) is equal to -1 if

$$E_{\rm F} + \omega < y < E_{\rm F}\ \ and\ \ \sqrt{(k-q)^2+\Delta^2} < y < \sqrt{(k+q)^2+\Delta^2} \tag{B5}$$

As what we did before, we calculate overlap between intervals and thus we find $q > k - k_{\rm F}$ and $q < k + k_{\rm F}$, $q > \sqrt{\omega^2+k_{\rm F}^2+2\omega\sqrt{k_{\rm F}^2+\Delta^2}} - k$. Putting everything together and using the fact that $q \geq 0$ we finally find

$$\begin{aligned}\Sigma^{res}_{intra}(\mathbf{k},\Delta-E_{\rm F}<\omega<0) &= -\frac{e^2}{2\pi\kappa\sqrt{k^2+\Delta^2}}\int_{max(0,k-k_{\rm F},\sqrt{\omega^2+k_{\rm F}^2+2\omega\sqrt{k_{\rm F}^2+\Delta^2}}-k)}^{k+k_{\rm F}} dq \\ &\times\ \int_{max(0,\omega+\sqrt{k_{\rm F}^2+\Delta^2},\sqrt{(k-q)^2+\Delta^2})}^{min(\sqrt{k_{\rm F}^2+\Delta^2},\sqrt{(k+q)^2+\Delta^2})} dy \\ &\times\ \frac{(\sqrt{k^2+\Delta^2}+y)^2-q^2}{\epsilon(\mathbf{q},\omega+E_{\rm F}-y)\sqrt{4k^2q^2-(y^2-k^2-q^2-\Delta^2)^2}}\end{aligned} \tag{B6}$$

$$\Sigma^{res}_{intra}(\mathbf{k},\omega<-\Delta-E_{\rm F}) = -\frac{e^2}{2\pi\kappa\sqrt{k^2+\Delta^2}}\int_{max(0,k-k_{\rm F})}^{k+k_{\rm F}} dq \int_{max(0,\omega+\sqrt{k_{\rm F}^2+\Delta^2},\sqrt{(k-q)^2+\Delta^2})}^{min(\sqrt{k_{\rm F}^2+\Delta^2},\sqrt{(k+q)^2+\Delta^2})} dy \times \frac{(\sqrt{k^2+\Delta^2}+y)^2-q^2}{\epsilon(\mathbf{q},\omega+E_{\rm F}-y)\sqrt{4k^2q^2-(y^2-k^2-q^2-\Delta^2)^2}} \quad \text{(B7)}$$

The real and imaginary part of intraband contributions can be computed.

APPENDIX C: THE INTERBAND CONTRIBUTION OF SELF-ENERGY

Now, we focus on the interband contribution of the retarded self-energy. The second argument of the dielectric function in Eq. (5) is

$$\omega-\xi_-(\mathbf{k}+\mathbf{q}) = \omega+E_{\rm F}+\sqrt{k^2+q^2+2kq\cos\phi+\Delta^2}\ . \quad \text{(C1)}$$

We change variable $y=\sqrt{k^2+q^2+2kq\cos\phi+\Delta^2}$, then we find

$$\Sigma^{res}_{inter}(\mathbf{k},\omega) = \frac{e^2}{2\pi\kappa\sqrt{k^2+\Delta^2}}\int_0^{+\infty} dq \int_{\sqrt{(k-q)^2+\Delta^2}}^{\sqrt{(k+q)^2+\Delta^2}} \frac{dy}{\sqrt{4k^2q^2-(y^2-k^2-q^2-\Delta^2)^2}} \frac{q^2-(y-\sqrt{k^2+\Delta^2})^2}{\epsilon(\mathbf{q},\omega+E_{\rm F}+y)} \times [\Theta(\omega+E_{\rm F}+y)-1]. \quad \text{(C2)}$$

Note that Σ^{res}_{inter} can be non-zero if $\omega+E_{\rm F}+y<0$ *and* $y>0$. It means that $\omega<-E_{\rm F}$. In this case the difference between the two Θ-functions in Eq. (5) becomes -1 if

$$0<y<-(\omega+E_{\rm F}) \ \ and \ \ \sqrt{(k-q)^2+\Delta^2}<y<\sqrt{(k+q)^2+\Delta^2}\ . \quad \text{(C3)}$$

Now we do need to find the overlap between these two intervals. We end up to inequivalent conditions that $q>k-\sqrt{\omega^2+k_{\rm F}^2+2\omega\sqrt{k_{\rm F}^2+\Delta^2}}$ and $q<k+\sqrt{\omega^2+k_{\rm F}^2+2\omega\sqrt{k_{\rm F}^2+\Delta^2}}$. Putting everything together and using the fact that $q\geq 0$ we finally get

$$\Sigma^{res}_{inter}(\mathbf{k},\omega<-E_{\rm F}) = -\frac{e^2}{2\pi\kappa\sqrt{k^2+\Delta^2}}\int_{max(0,k-\sqrt{\omega^2+k_{\rm F}^2+2\omega\sqrt{k_{\rm F}^2+\Delta^2}})}^{k+\sqrt{\omega^2+k_{\rm F}^2+2\omega\sqrt{k_{\rm F}^2+\Delta^2}}} dq \int_{\sqrt{(k-q)^2+\Delta^2}}^{min(\sqrt{(k+q)^2+\Delta^2},-(\omega+\sqrt{k_{\rm F}^2+\Delta^2}))} dy \times \frac{q^2-(y-\sqrt{k^2+\Delta^2})^2}{\epsilon(\mathbf{q},\omega+\varepsilon_{\rm F}+y)\sqrt{4k^2q^2-(y^2-k^2-q^2-\Delta^2)^2}}. \quad \text{(C4)}$$

If we want to calculate $\Im m\Sigma^{res}_{+}(\mathbf{k},\xi_+(\mathbf{k}))$ needed for computing the quasiparticle lifetime, we will only need the intraband contribution of the self-energy since the interband contribution is zero.

[1] K. S. Novoselov, A. K. Geim, S. V. Morozov, D. Jiang, Y. Zhang, S. V. Dubonos, I. V. Grigorieva, A. A. Firsov, Science **306**, 666 (2004); K. S. Novoselov, A. K. Geim, S. V. Morozov, D. Jiang, M. I. Katsnelson, I. V. Grigorieva, S. V. Dubonos and A. A. Firsov, Nature **438**, 197 (2005); K. S. Novoselov, D. Jiang, F. Schedin, T. J. Booth, V. V. Khotkevich, S. V. Morozov, and A. K. Geim, Proc. Nat. Acad. Sci. **102**, 10451 (2005) .

[2] Andreas Barth, Werner Marx, arXiv:0808.3320 (2008) .

[3] A. A. Balandin, S. Ghosh, W. Bao, I. Calizo, D. Teweldebrhan, F. Miao, C. N. Lau, Nano Lett., **8**, 902 (2008) .

[4] S.V. Morozov, K.S. Novoselov, M.I. Katsnelson, F. Schedin, D.C. Elias, J.A. Jaszczak, A.K. Geim, Phys. Rev. Lett. **100**, 016602 (2008); K. I. Bolotin, K. J. Sikes, J. Hone, H. L. Stormer, and P. Kim, Phys, Rev, Lett. **101**, 096802 (2008); Xu Du, Ivan Skachko, Anthoy Barker and Eva Y. Andrei, Nature Nanotech. **3**, 491 (2008); K.I. Bolotin, K.J. Sikes, Z. Jiang, M. Klima, G. Fudenberg, J. Hone, P. Kim, H.L. Stormer, Solid State Commun. **146**, 351 (2008) .

[5] K. Eng, R. N. McFarland, and B. E. Kane, Appl. Phys. Lett. **87**, 052106 (2005); E. H. Hwang and S. Das Sarma, Phys. Rev. B **75**, 073301 (2007) .

[6] T. O. Wehling, K. S. Novoselov, S. V. Morozov, E. E. Vdovin, M. I. Katsnelson, A. K. Geim, A. I. Lichtenstein, Nano Lett. **8**, 173-177 (2008); S.Y. Zhou, D.A. Siegel, A.V. Fedorov, A. Lanzara, Phys. Rev. Lett. **101**, 086402 (2008); Isabella Gierz, Christian Riedl, Ulrich Starke, Christian R. Ast, Klaus Kern, arXiv:0808.0621 .

[7] S. Y. Zhou, G. H. Gweon, A. V. Federov, P. N. First, W. A. de Heer, D. H. Lee, F. Guinea, A. H. Castro Neto, and A. Lanzara, Nat. Mater. **6**, 770 (2007) .

[8] G. Li, A. Luican, and E. Y. Andrei, arXiv:0803.4016 (2008) .

[9] Gianluca Giovannetti, Pet A. Khomyakov, Geert Brocks, Paul J. Kelly, and Jeoroen Van den Brink, Phys. Rev. B **76**, 073103 (2007) .

[10] R. M. Ribeiro, N. M. R. Peres, J. Coutinho, and P. R. Briddon, Phys. Rev. B **78**, 075442 (2008) .

[11] I. Zanella, S. Guerini, S. B. Fagan, J. Mendes Filho, and A. G. Souza Filho, Phys. Rev. B **77**, 073404 (2008) .

[12] Yugui Yao, F. Ye, Xiao-Liaug Qi, Shou-Cheng Zhang and Zhang Fang, Phys. Rev. B **75**, 041401(R) (2007); C. L. Kane, and E. J. Mele, Phys. Rev. Lett. **95**, 226801 (2005); Hongki Min, J. E. Hill, N. A. Sinitsyn, B. R. Sahu, Leonard Kleinman, and A. H. MacDonald, Phys. Rev. B **74**, 165310 (2006) .

[13] Y. W. Son, M. L. Cohen, and S. G. Louie, Phys. Rev. Lett. **97**, 216803 (2006); M. Y. Han, B. Ozyilmaz, Y. Zhang, and P. Kim, *ibid* **98**, 206805 (2007) .

[14] L.D. Landau, Sov. Phys. JEPT, **3**, 920 (1957) .

[15] I.K. Marmorkos and S. Das Sarma, Phys. Rev. B **44**, R3451 (1991); J.D. Lee and B.I. Min, Phys. Rev. B **53**, 10 988 (1996); H.-J. Schulze, P. Schuck, and N. Van Giai, Phys. Rev. B **61**, 8026 (2000) .

[16] S. Yarlagadda and G.F. Giuliani, Phys. Rev. B **49**, 7887 (1994); **61**, 12556 (2000); C.S. Ting, T.K. Lee, and J.J. Quinn, Phys. Rev. Lett. **34**, 870 (1975).

[17] H. M. Böhm and K. Schörkhuber, J. Phys.: Condens. Matter **12**, 2007 (2000) .

[18] Y. Zhang and S. Das Sarma, Phys. Rev. B **71**, 045322 (2005); S. Das Sarma, V. M. Galitski, and Y. Zhang, Phys. Rev. B **69**, 125334 (2004) .

[19] Y. Zhang, V.M. Yakovenko, and S. Das Sarma, Phys. Rev. B **71**, 115105 (2005) .

[20] R. Asgari, B. Davoudi, M. Polini, Gabriele F. Giuliani, M. P. Tosi, and G. Vignale, Phys. rev. B **71**, 045323 (2005); R. Jalabert and S. Das Sarma, Phys. Rev. B **40**, 9723 (1989) .

[21] R. Asgari, B. Davoudi and B. Tanatar, Solid State Commun. **130**, 13 (2004).

[22] Jahan M. Dawlaty, Shriram Shivaraman, Mvs Chandrasekhar, Farhan Rana, Micheal G. Spencer, App. Phys. Lett **92**, 042116 (2008) .

[23] J. R. Williams, L. DiCarlo and C. M. Marcus Since **317**, 638 (2007) .

[24] G. Gu, S. Nie, R. M. Feenstra, R. P. Devaty, W. J. Choyke, W. K. Chan and M. G. Kane, Appl. Phys. Lett. **90**, 253507 (2007) .

[25] Marco Polini, Reza Asgari, Giovanni Borghi, Yafis Barlas, T. Pereg-Barnea, and A.H. MacDonald, Phys. Rev. B **77**, 081411(R) (2008); E. H. Hwang and S. Das Sarma, Phys. Rev. B **77**, 081412(R) (2008) .

[26] Z. Q. Li, E. A. Henriksen, Z. Jiang, Z. Hao, M. C. Martin, P. Kim, H. L. Stromer, D. N. Basov, Nature Phys. **4**, 532 (2008) .

[27] M. Polini, R. Asgari, Y. Barlas, T. Pereg-Barnea, A. H. MacDonald, Solid State Commun. **143**, 58 (2007) .

[28] G. F. Giuliani and G. Vignale, *Quantum Theory of The Electron Liquid* (Cambridge University Press, Cambridge, England, 2005).

[29] A. Qaiumzadeh and R. Asgari, arXiv:0807.3183 (2008) .

[30] P. K. Pyatkovskiy, arXiv:0808.0931 (2008) .

[31] E. H. Hwang, BenYu-Kaung Hu, and S. Das Sarma, Phys. Rev. B **76**, 115434 (2007) .

[32] R. Asgari and B. Tanatar, Phys. Rev. B 65 (2002) 085311 .

[33] Y. Barlas, T. Pereg-Barnea, M. Polini, R. Asgari and A. H. MacDonald, Phys. Rev. Lett. 98 (2007) 236601 .

[34] A. Qaiumzadeh, N. Arabchi, R. Asgari, Solid State Commun. **147**, 172 (2008) .

[35] G.F. Giuliani and J. J. Quinn, Phys. Rev. B **26**, 4421 (1982) .

[36] P. K. Pyatkovskiy, Private communication .

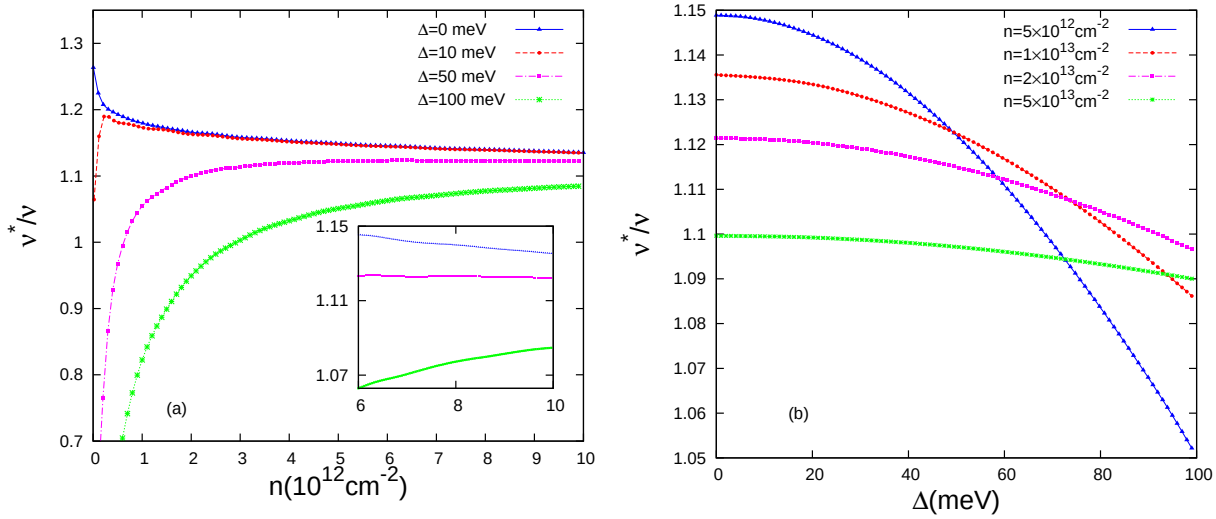

FIG. 1: (Color online) (a): The renormalized velocity as a function of density for the various energy gaps at $\alpha_{gr} = 1$. (b): The renormalized velocity as a function of the energy gap for the various densities.

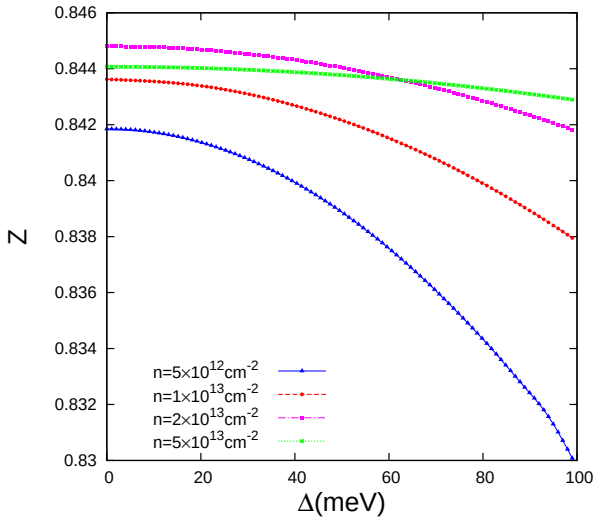

FIG. 2: (Color online) The renormalization constant as a function of the energy gap for the various densities.

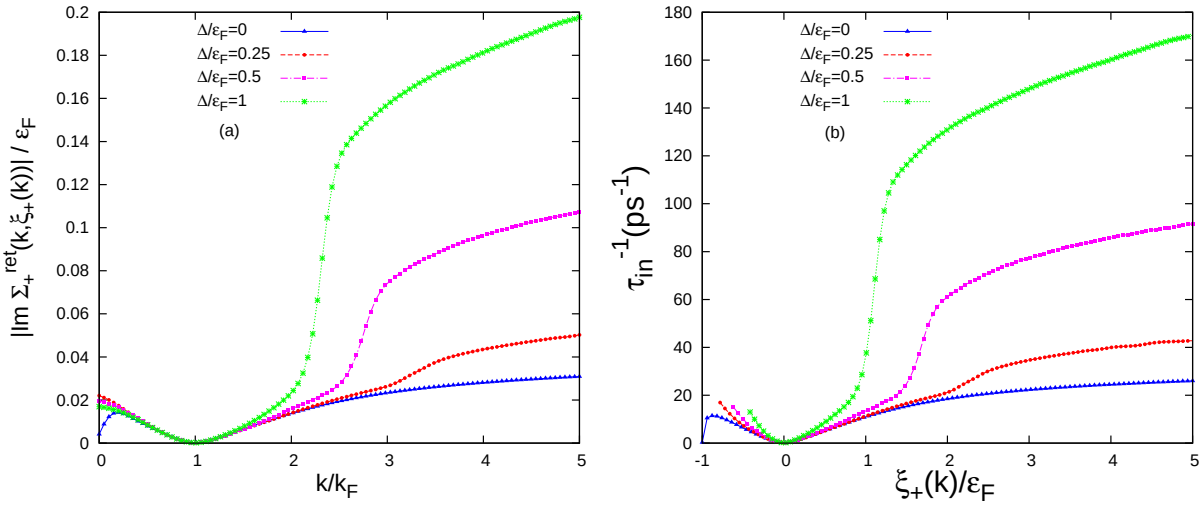

FIG. 3: (Color online) (a): The absolute value of the imaginary part of the retarded self-energy on the energy shell as a function of the wavevector for the various energy gaps; (b): The inelastic quasiparticle lifetime(τ_{in}) in graphene as a function of the on-shell energy for the various energy gaps at $n = 5 \times 10^{12}\text{cm}^{-2}$.

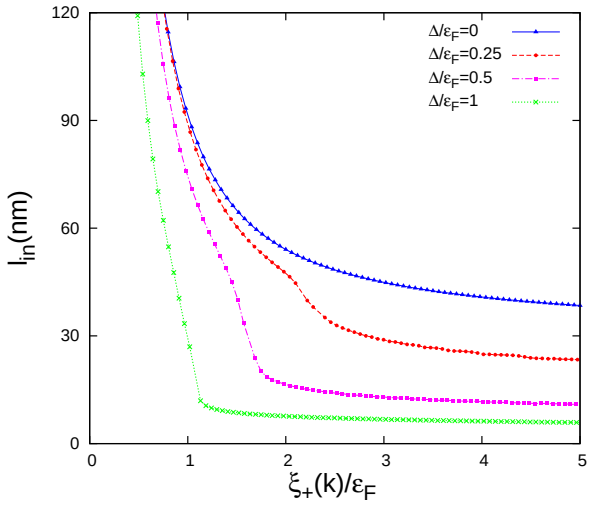

FIG. 4: (Color online) The quasiparticle mean free path as a function of the on-shell energy for the various energy gaps at $n = 5 \times 10^{12}\text{cm}^{-2}$.